Journal of Applied Biology & Biotechnology Vol. 11(Suppl 1), pp. 40-45, December, 2023
Available online at http://www.jabonline.in
DOI: 10.7324/JABB.2023.145826

Preparation of zinc oxide-carboxymethyl cellulose blended with cyclophosphamide for targeted drug delivery to lung adenocarcinoma cells

K. Harsha Prabha, Mahalakshmi Nannan, Sivaramakrishnan Venkatabalasubramanian*

Department of Genetic Engineering, College of Engineering and Technology, SRM Institute of Science and Technology, Kattankulathur Campus, Chennai-603203, Tamil Nadu, India.

ARTICLE INFO

Article history:
Received on: August 09, 2023
Accepted on: November 05, 2023
Available online: December 15, 2023

Key words:
Polymeric nanocomposites,
Lung cancer,
Cyclophosphamide,
Carboxymethyl cellulose,
Zinc oxide.

ABSTRACT

Lung adenocarcinoma represents more than 40% of global lung cancer cases diagnosed yearly. Nano-drug delivery systems made from polymeric nanocomposites (NCs) have been described as promising carriers of chemotherapeutic payload against lung adenocarcinoma. Zinc oxide (ZnO) nanoparticles, which have been shown to produce tumor-selective cell death, lower treatment resistance, and lower side effects *in vitro*, are excellent therapeutic systems that can be combined with chemotherapeutic agents. Using the chemical reduction method, we prepared ZnO nanoparticles in this study and embedded them in non-toxic adsorbent carboxymethyl cellulose (CMC). This polymeric nanocomposite (NC) was further blended with cyclophosphamide (CPS): A hydrophobic chemotherapeutic drug and analyzed for its cytotoxicity against lung adenocarcinoma cells. Characterization of NCs was performed by UV-visible spectroscopy, dynamic light scattering, Fourier-transform-infrared spectroscopy, and transmission electron microscopy. MTT analysis revealed that the biological cytotoxic potential of ZnO-CMC-CPS NCs was superior to ZnO-CMC NCs against A549 cells. Furthermore, Western blot analysis for Ki-67 (proliferation biomarker) expression analysis was performed for ZnO entrapped CMC NC versus ZnO-CMC-CPS-treated lung adenocarcinoma cells. ZnO-CMC-CPS NCs revealed a superior decrease in Ki-67 expression compared to ZnO-CMC alone treated lung adenocarcinoma cells. These results indicate that the synthesized ZnO-CMC-CPS polymeric NC, compared to ZnO-CMC, is an efficient drug delivery system with anti-proliferative potential and augmented cytotoxicity against lung adenocarcinoma cells. These polymeric NCs are prospective drug delivery systems for antiproliferative therapy.

ARTICLE HIGHLIGHTS

1. Preparation of ZnO with Carboxymethyl Cellulose (CMC) polymer as nanoparticles.
2. Synthesis of ZnO-CMC and cyclophosphamide(CPS) nanocomposites showed cytotoxicity against A549 cells.
3. Ki-67 expression decreased on treating the A549 cells with ZnO-CMC-CPS nanocomposite.

1. INTRODUCTION

Cancer is the second leading cause of death in the world. Lung cancer is highly invasive and metastasizes to other body parts, such as the lymph glands and breasts. Smoking and tobacco use are significant risk factors for 90% of lung cancer cases. The additional risk factors include environmental and genetic factors. Histologically, lung cancer can be categorized into small-cell lung cancer and non-small cell lung cancer (NSCLC). It is one of the major causes of cancer-associated death worldwide, and approximately 85% of lung cancer cases are NSCLC [1-3]. Standard cancer therapies include chemotherapy, immunotherapy, hormone therapy, radiation therapy, and surgery. Anticancer drugs other than monoclonal conjugated antibody-based drugs used to target cancer cannot distinguish between normal and cancerous cells, leading to off-target binding and severe side effects [4,5]. The primary aim of developing anticancer agents is to improve drug targets and delivery to the tumor without affecting normal cells.

Nanoscience technology has provided strategies for the precise delivery of therapeutic drugs to tumors for effective treatment [6,7]. Nanocomposites (NCs) have a size range of 10–1000 nm. Owing to their small size, they have unique biological properties. NCs contain two or more components. They can be either organic or inorganic compounds coupled to one another. Many NCs with

*Corresponding Author:
Dr. Sivaramakrishnan Venkatabalasubramanian,
Department of Genetic Engineering,
Faculty of Engineering and Technology,
SRM Institute of Science and Technology,
Kattankulathur, Chennai - 603 203, Tamil Nadu, India.
Phone: +91-9444931980, E-mail: svrmkrish@gmail.com

practical evidence-based specificity can target tumors [8-10]. Oncology-based nanotechnology provides opportunities for site-specific drug delivery, improved drug stability, increased drug conjugation capacity, and enhanced targeting of cancer cells by drug modification. Loading the desired drug as payload in the nanocarrier system is performed by (i) incorporation method: Incorporation of the drug of interest during NC formation. (ii) adsorption method: The required drug concentration could be loaded and incubated after preparing the nano-formulation. Such nano-formulations of drug molecules can cross the blood–brain barrier and be used to treat brain tumors [11,12]. Nanocarriers have the potential to accumulate therapeutic agents at tumor and inflammatory sites. After accumulation, nanocarriers release the drug slowly into the tissue site. Many types of nanocarrier systems are used to target cancer cells. They include dendrimers, liposomes, carbon nanotubes, metal-polymer NCs, and magnetic nanocarriers [13] [Table 1].

The two main properties of polymer NCs are their small size and biodegradability. Biopolymers, such as carboxymethyl cellulose (CMC), have gained attention among researchers because they easily bind to the biological membrane and penetrate the mucous layer. CMC is a water-soluble, negatively charged cellulose derivative [14-18]. The human enzyme system can efficiently digest the biopolymer CMC. Their efficient drug bioavailability enhances their anticancer effects with low immunogenicity. It comprises plant tissue fibers and a long linear chain of sodium carboxymethyl groups (CH2COONa). Among the biopolymers, CMC is readily available and cost-effective. CMC offers a platform for entrapping the metal ions to form biopolymer-metal NCs.

Zinc oxide (ZnO), which belongs to the class of metal oxides, has potential applications in piezoelectric nanogenerators, optoelectronics, and pharmaceutical biotechnology products. Nano-sized ZnO upregulates the tumor suppressor gene p53 and pro-apoptotic genes (Bax) corresponding to mitochondrial independent and dependent pathways. Nonetheless, they also suppress the anti-apoptotic (Bcl-2) signaling pathway. In addition, ZnO attacks the tumor by generating reactive oxygen species (ROS) and activates the caspase pathways with induced apoptosis [19-21]. The most common and oldest family of chemotherapy medications is "alkylating agents," which add an alkyl group to the DNA double helix to impede DNA replication and ultimately prevent cell proliferation. One of the most effective anticancer medications is cyclophosphamide (CPS), an alkylating agent. Phosphoramide mustard is produced when microsomal liver enzymes such as cytochrome P-450 metabolize CPS. It is primary mechanism of action includes interacting with proteins that control cellular biological processes to prevent or limit cellular proliferation, directly impairing DNA synthesis, or inhibiting DNA transcription. Nevertheless, it possesses dose-dependent side effects, hence toxicity [22,23]. Especially long-term treatment and large dosages of CPS should be avoided whenever feasible [24]. In this context, biopolymer CMC with metal oxide ZnO entrapment enabled the formation of ZnO-CMC NCs with the latent abrogation of tumor DNA and proliferation. In addition, ZnO-CMC NCs blended with the anticancer drug CPS were checked for their effective cytotoxicity against A549 (NSCLC) cells. This study provides a detailed analysis of the synthesis, characterization, and biological evaluation of ZnO-CMC and ZnO-CMC-CPS NCs.

2. MATERIALS AND METHODS

All the reagents and chemicals used in this study were of analytical grade. MTT (3-[4,5-dimethylthiazol-2-yl]-2,5-diphenyltetrazolium bromide), CMC, and ZnO were purchased from SISCON Pvt. Ltd. (India). CPS was purchased from Zydus Cadila Pharmaceuticals Pvt. Ltd. (India). NSCLC cell line (A549) was purchased from the National Repository (NCCS), Pune, and cultured at the SRM Institute of Science and Technology. The A549 (epithelial lung adenocarcinoma) cells were maintained in Dulbecco's Modified Eagle Medium (DMEM) containing 10% fetal bovine serum and 1% penicillin/streptomycin with a 5% supply of CO_2 at 37°C.

2.1. Synthesis of ZnO-CMC NCs

The chemical reduction method was applied to synthesize ZnO-CMC NCs [Figure 1]. First, CMC (0.06 g) was dissolved in 10 mL of distilled water, followed by ZnO (0.1 g). To dissolve CMC completely, the solution was heated at 90°C for 15 min under constant stirring, and the mixture was cooled to room temperature. The ZnO and CMC solutions were sonicated in a bath sonicator for 25 min. The ZnO solution was added dropwise to the CMC solution with a magnetic stirrer until the transparent mixture turned milky white. The mixture was centrifuged at 8000 rpm for 20 min. The supernatant was discarded, and the pellet contained ZnO-CMC NCs. To get rid of other compounds, the NCs were washed with distilled water, and the NCs pellet was dried at 45°C for 1 h using a vacuum concentrator for the next step.

2.2. CPS Blending with ZnO-CMC NCs

Coat the outer surface of the ZnO-CMC NCs with the anticancer drug CPS. The prepared ZnO-CMC NCs (500 µL) were mixed with 500 µL CPS solution and incubated for1h at room temperature. The suspension was then centrifuged at 8000 rpm for 15 min. The pellet contained the ZnO-CMC/CPS NCs. The sample was dried using a vacuum concentrator set at 45°C for an hour.

2.3. Characterization

The synthesized ZnO-CMC and ZnO-CMC-CPS NCs were analyzed using a UV-visible spectrophotometer. This is the primary characterization technique used to check the aggregation and particle distribution of the NCs. The sample was analyzed in the 200–1100 nm absorbance range using Thermo Fisher's GENESYS 150. Fourier-transform-infrared spectroscopy (FT-IR) was analyzed using a Shimadzu infrared tracer-100 to investigate the functional groups

Table 1: Different types of nanocarriers used in cancer therapy.

Nanocarrier	Size	Uses	References
Dendrimers	5–20 nm	Cancer diagnosis, photodynamic therapy	[28,29]
Liposomes	30 nm–10 µm	Site-specific drug delivery. It also improves the stability of the drug	[30,31]
Metal-polymer nanocomposites	10–1000 nm	Passive drug delivery and high drug concentration. Low toxicity	[32]
Carbon nanotube	0.4–3 nm	Facilitates cancer cell destruction	[33,34]
Magnetic nanocarrier	70–140 nm	Magnetic resonance imaging	[35,36]

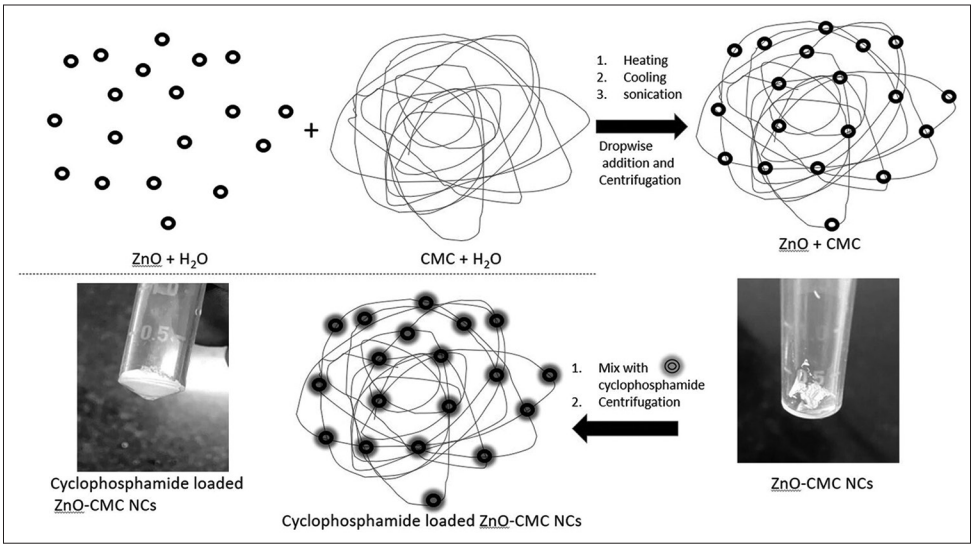

Figure 1: Synthesis of zinc oxide-carboxymethyl cellulose nanocomposites and cyclophosphamide-loaded nanocomposites.

present in the NCs and CPS-coupled NCs within the transmission frequency range from 400 cm^{-1} to 4000 cm^{-1} at a resolution of 2 cm^{-1}. This study used dynamic light scattering (DLS) to determine the size and explains the hydrodynamic diameter of the prepared NCs at a scattering angle of 90°C using Horiba Scientific, SZ-100. The standard volume cuvette (3.5 mL) was used in the analysis. Transmission electron microscopy (TEM) analysis was used to identify the morphology of the NCs. The carbon-supported copper grid with a mesh size of 3 mm was used to evaluate each sample. X-ray diffractometer (Bruker USA D8 advance, Davinci) was used to analyze lattice parameters and the crystalline structure of the nanoparticle.

2.4. MTT Assay

In a 96-well tissue culture plate, NSCLC (A549) cells were seeded at a 5 × 10^{-3} density and maintained in DMEM. Then, the ZnO-CMC-CPS NCs were added to five different concentrations (10, 50, 100, 250, and 500 µM) and incubated for 24 h. Before completing the experiment, 50 µL of MTT reagent was added and incubated at 37°C in a CO2 incubator for 4 h. A 100 µL of 0.1% dimethyl sulfoxide was added to dissolve formazan crystal. Absorbance was measured using a microplate reader at a wavelength of 570 nm. All samples were analyzed in triplicate to determine the metabolic activity of the cells.

2.5. Western Blotting

Expression of Ki-67 and β-actin levels was assessed by western blotting. A 50 mg of protein was loaded after boiling it with Laemmli buffer at 95°C for 5 min, and proteins were separated by sodium dodecyl-sulfate polyacrylamide gel electrophoresis (10%) at room temperature. It was blotted onto the polyvinylidene fluoride membrane and was then blocked with 5% skimmed milk in phosphate-buffered saline (PBS) with 0.2% to 20 (PBS-T) at room temperature for one h and probed with primary antibodies diluted in PBS-T: Anti-Ki-67, anti-β-actin mouse monoclonal antibody (1:1000 dilution of each) overnight at 4°C. The membranes were washed gently with diluted PBS-T and incubated with anti-mouse secondary antibodies linked to horse-radish peroxidase at a 1:5000 dilution for 1 h. Reactive bands were detected using enhanced chemiluminescence and quantified. β-actin was used as an endogenous control to check for equal sample loading.

3. RESULTS AND DISCUSSION

3.1. Synthesis of NCs

Our studies revealed that white-colored nanoparticles were formed when ZnO was entrapped with a transparent solution of CMC under constant stirring. Furthermore, mixing with CPS and centrifugation resulted in a dried white-colored pellet of ZnO-CMC-CPS NCs [Figure 1].

3.2. UV-Visible Spectroscopy Analysis of Synthesized ZnO-CMC NCs

The highest absorbance peak of the ZnO-CMC NCs was observed at 260 nm. The absorbance values obtained were 1.286 (398 nm) and 1.187 (514 nm), respectively [Supplementary Figure and Table 1]. The polydispersity index (PDI) measures the molecular mass distribution of the sample. It can be calculated as the ratio of weight average to number average size or molecular weight. PDI values may range from 0 to 2, with lower values indicating a narrower distribution and higher values indicating a wider distribution. The ZnO-CMC NC appears to have a lower PDI value. This further confirmed the monodisperse distribution of the NCs.

3.3. DLS Analysis

The hydrodynamic diameter of NC under monodisperse distribution was obtained at 25°C. The size of the NC ranges between 129.4 nm and 698.4 nm [Supplementary Figure 2a and b] of ZnO-CMC and ZnO-CMC-CPS NCs, respectively. The presence of a single peak demonstrates a homogeneous distribution of the particles. A 10–1000 nm is the usual range of the NC. The hydrodynamic diameters of ZnO-CMC and ZnO-CMC-CPS NCs were within the nano range based on our analysis. Furthermore, our results corroborate well with previous findings by another group [25], suggesting that the hydrodynamic diameter of ZnO-CMC NCs lies within the range of 100–200 nm. The hydrodynamic diameter [Table 2] of ZnO-CMC-CPS NCs was observed as 698.4 nm, which is higher than the ZnO-CMC NCs due to the presence of CPS. This analysis confirmed the addition of CPS to the NCs.

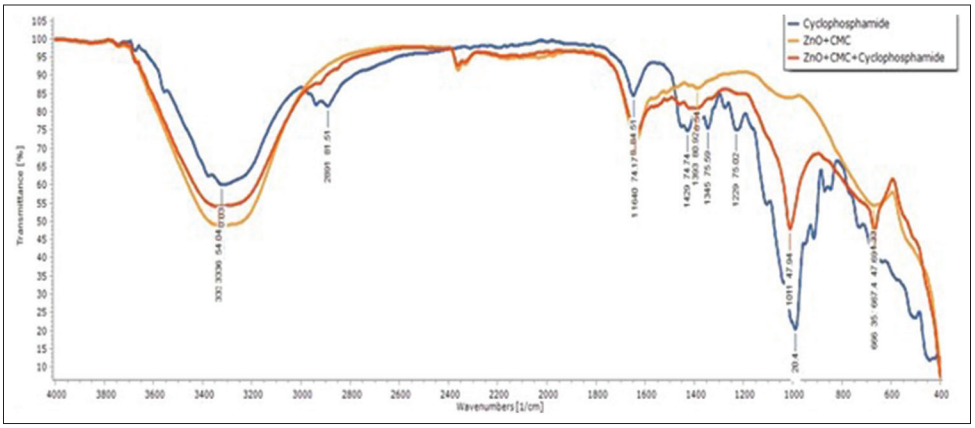

Figure 2: Fourier-transform-infrared spectra of cyclophosphamide, zinc oxide (ZnO)-carboxymethyl cellulose nanocomposites (NCs), ZnO-carboxymethyl cellulose/cyclophosphamide NCs.

Table 2: Results of DLS analysis.

S. No.	Sample	Z-average (nm)	PDI
1	ZnO-CMC NCs	129.4	1.264
2	ZnO-CMC-CPS NCs	698.4	1.485

DLS: Dynamic light scattering, PDI: Polydispersity index

3.4. FT-IR Analysis

IR spectra [Figure 2] show the ZnO-CMC and ZnO-CMC-CPS NCs. The peaks formed at 3383.2 cm^{-1}, 1694.4 cm^{-1}, and 500–400 cm^{-1} reveal the spectrum of ZnO-CMC NCs. FT-IR spectra [Figure 2] also depict the ZnO-CMC-CPS NCs formed at 3383.2 cm^{-1}, 1694.4 cm^{-1}, and 1000 cm^{-1}–500 cm^{-1}, respectively. The peak formed at 3383.2 cm^{-1} represents the -OH functional group, indicating the presence of water molecules. The small characteristic peak at 1695.4 cm^{-1} is due to the -COOH stretching vibration, which corresponds to the presence of CMC. Our results corroborate the findings of Luna-Martínez *et al.* [26], suggesting a similar peak value for CMC. A sharp peak is also observed at 500–400 cm^{-1}, indicating the presence of ZnO. Awan *et al.* [27] showed that the peak for ZnO forms between 430 and 500 cm^{-1}. Comparing the spectrum peaks [Figure 2], there is a shift in the peak from 1000 cm^{-1} to 500 cm^{-1}, indicating the presence of the amide functional group in CPS [Table 3]. Therefore, based on the FT-IR results, it is clear that CPS is coupled with the CMC of the ZnO NC through amide functional group interactions.

3.5. TEM Analysis

The morphological study of the ZnO metal oxide was analyzed using TEM analysis. The biopolymer [Figure 3a] CMC is a thread and fibrous-like structure. The patch-like structural design [Figure 3b] present in the fibrous mesh of CMC represents the entrapped ZnO nanoparticles. Much denser aggregates of CPS were also observed scattered and blended in the NCs. The data from TEM analysis further confirmed the observation of the DLS analysis that the nano-size range of the ZnO-CMC NCs remained between 100 and 200, which increased to 600–700 nm in size when blended with CPS.

3.6. XRD Analysis

ZnO NPs exhibited a wurtzite-like structure and were hexagonal [Figure 4] with the planes of the crystal (100), (002), (101), (102), and (110) and the diffraction peaks with 20 values of 31.73°, 34.52°, 36.33°, 47.74°, and 56.78°, respectively. The result has no other diffraction peak indicating the ZnO nanoparticle's purity. This analysis was only performed to provide overwhelming confirmatory evidence on the presence of metal oxide in the NCs, particularly ZnO. Since CMC or CPS does not involve the existence of any metal atoms, XRD analysis was not performed.

Table 3: The FT-IR spectra of ZnO-CMC-CPS NCs.

S. No.	Wave number (cm^{-1})	Functional group
1	1010.70	Aromatic C-H in-plane bend
2	667.37	Aromatic C-H out of the plane bend
3	2362.8	C≡H bond
4	1639.49	Alkenyl C=C

FT-IR: Fourier transform infrared

3.7. MTT Assay

Five different concentrations (10–500 µM) of ZnO-CMC-CPS NCs were compared with ZnO-CMC alone. The mean % cell viability of ZnO-CMC-CPS NCs ranged between 85.96% and 36.84% against A549 cells [Figure 5]. However, the mean % cell viability of ZnO-CMC alone at the same concentrations ranged from 65.24% to 45%. There was a significant reduction in the viability of A549 cells treated with either ZnO-CMC-CPS NCs or ZnO-CMC alone. The results indicate that superior augmented cytotoxicity was observed at higher concentrations of ZnO-CMC-CPS NCs than with ZnO-CMC alone. Compared to the control, the cell proliferation of A549 cells decreased from 14.04% to 63.16% with increasing concentrations (10 µM–500 µM) of the ZnO-CMC-CPS NCs, respectively. On the contrary, ZnO-CMC alone decreased cell proliferation much slower than ZnO-CMC-CPS NCs. CMC is a perfect biopolymer that serves as a fibrous mesh platform to aggregate the ZnO (metal oxide) and CPS (chemotherapeutic drug). ZnO is known to generate excess ROS, killing cancer cells. In addition, CPS is an alkylating anticancer agent that attacks and destroys only the rapidly proliferating tumor cells. The results from the MTT analysis indicated that when A549 cells were incubated with ZnO-CMC-CPS rather than ZnO-CMC NCs, the cell proliferation rate declined rapidly at increasing concentrations. This suggests their superior prospective synergistic cytotoxicity potential compared to ZnO-CMC alone against lung adenocarcinoma (A549) cells.

3.8. Westernblot Analysis

Ki-67 is a categorical proliferation marker. It is increased expression indicates higher proliferation and aggressive cancer progression.

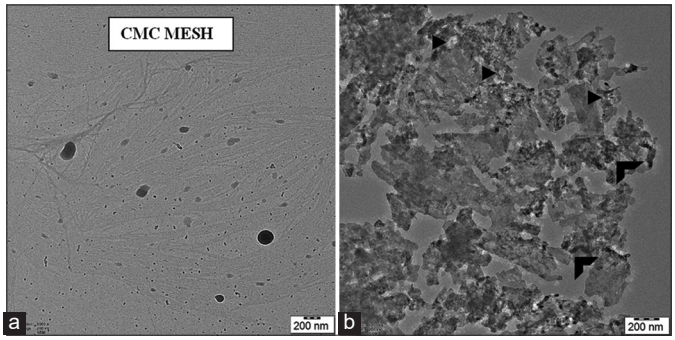

Figure 3: The transmission electron microscopy image of carboxymethyl cellulose (a) and Zinc Oxide (ZnO) NPs (ZnO represented as a black triangle) and cyclophosphamide (cyclophosphamide represented as a half frame) (b).

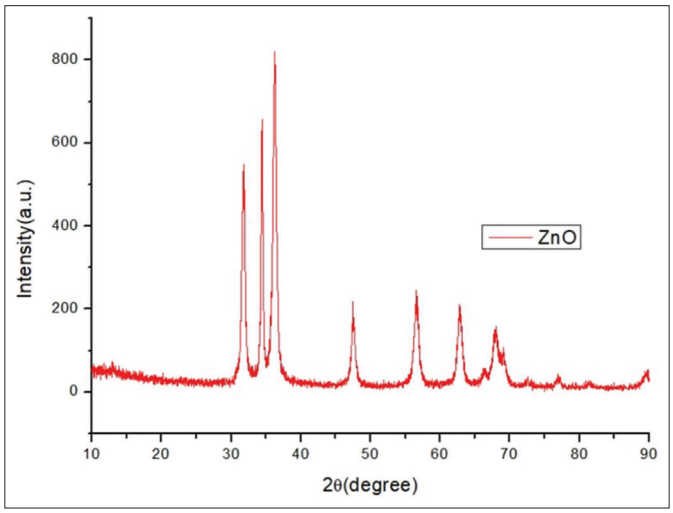

Figure 4: The X-ray powder diffraction image of zinc oxide nanoparticles.

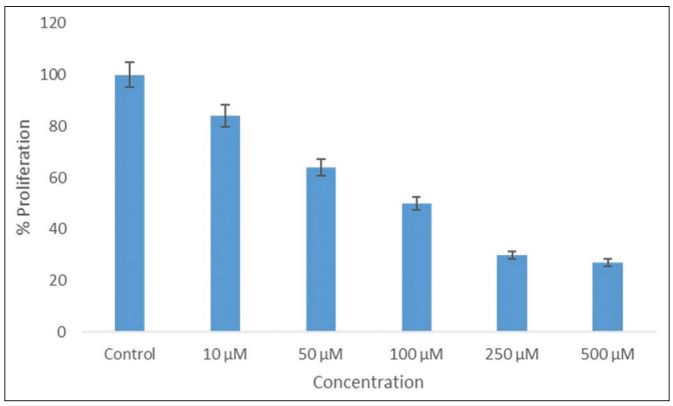

Figure 5: MTT assay analysis of synthesized zinc oxide-carboxymethyl cellulose-cyclophosphamide nanocomposites against A549 lung cancer cells.

Therefore, the expression levels of Ki-67 biomarker levels in A549 cells (control) treated with ZnO-CMC NPs, and ZnO-CMC-CPS NCM were ascertained in this study. In control lung adenocarcinoma (A549) cells, Ki-67 levels were significantly upregulated, suggestive of the high proliferation index of the cancer cells. However, ZnO-CMC-CPS compared to ZnO-CMC NCs-treated lung adenocarcinoma (A549) cells revealed an enhanced downregulation of Ki-67 expression, suggesting its anti-proliferative potential. The antiproliferative effects of both these NCs could be due to the enhanced release of ROS by

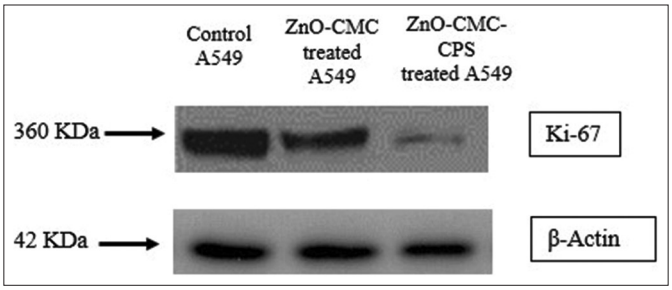

Figure 6: Representative immunoblots of Ki-67 and β-actin.

ZnO or the decreased proliferation by augmented susceptibility to anti-metabolites like CPS. The independent effects of ZnO-CMC-CPS NCs were superior in the down-regulation of Ki-67 expression in A549 cells compared to ZnO-CMC NCs alone [Figure 6]. This also suggests that the synergistic antiproliferative potential of ZnO-CMC blended with CPS NC is higher than ZnO-CMC NC alone when treated with lung adenocarcinoma (A549) cells.

4. CONCLUSION

The synthesized CPS-coupled ZnO-CMC NCs were stable and exhibited promising cytotoxicity against A549 cancer cells. As the ZnO-CMC NCs were small, they had a larger surface area. Hence, a higher concentration of CPS can be blended. The MTT assay results further demonstrated that the ZnO-CMC-CPS NCs effectively decreased the proliferation of A549 cells in a dose-dependent manner. The Western blot analysis for Ki-67 analysis irrevocably confirmed the anti-proliferative potential of the prepared NCs (ZnO-CMC and ZnO-CMC-CPS). This study suggests that combining NCs and chemotherapeutic drugs is a promising anticancer drug delivery strategy for targeting lung adenocarcinoma cells. Nevertheless, further understanding of the coupling efficiency of these nanometal composites, their sustained drug release, stability, and bioavailability is still nascent and requires further experimental exploration. Such studies should provide future perspectives for developing new combinations of polymeric NCs with ZnO and chemotherapeutic drugs to combat lung adenocarcinoma.

5. ACKNOWLEDGMENTS

The authors H, MN, and VSRK want to thank SRM IST for their constant motivation and support. We also thank the XRD and Nano-tech facilities at SRM IST for the infrastructure and technical support to perform the FT-IR, TEM, and DLS analysis.

6. AUTHORS' CONTRIBUTIONS

VSRK contributed to the conceptualization of the idea of this manuscript. H, MN, and VSRK contributed to the drafting and editing of the manuscript. All the authors have confirmed the integrity of the manuscript.

7. FUNDING

The study was not supported by any grant. This work was carried out under the SRM Institute of Science and Technology research programs.

8. CONFLICTS OF INTEREST

The authors report no financial or other conflicts of interest in this work.

9. ETHICAL COMPLIANCE

All procedures performed in studies do not involve human participants or clinical studies that might require following the ethical standards of the institutional and national research committee and with the 1964 Helsinki Declaration and its later amendments or comparable amendment's ethical standards.

10. DATA AVAILABILITY

This publication's research data and supporting information are available here and mentioned in the manuscript.

11. PUBLISHER'S NOTE

This journal remains neutral with regard to jurisdictional claims in published institutional affiliation.

REFERENCES

1. Sudhakar A. History of cancer, ancient and modern treatment methods. J Cancer Sci Ther 2009;1:1-4.
2. Lemjabbar-Alaoui H, Hassan OU, Yang YW, Buchanan P. Lung cancer: Biology and treatment options. Biochim Biophys Acta 2015;1856:189-210.
3. Wei MM, Zhou GB. Long non-coding RNAs and their roles in non-small-cell lung cancer. Genomics Proteomics Bioinformatics 2016;14:280-8.
4. Sadhukhan P, Kundu M, Chatterjee S, Ghosh N, Manna P, Das J, *et al*. Targeted delivery of quercetin via pH-responsive zinc oxide nanoparticles for breast cancer therapy. Mater Sci Eng C Mater Biol Appl 2019;100:129-40.
5. Sinha R, Kim GJ, Nie S, Shin DM. Nanotechnology in cancer therapeutics: Bioconjugated nanoparticles for drug delivery. Mol Cancer Ther 2006;5:1909-17.
6. Wang X, Yang L, Chen ZG, Shin DM. Application of nanotechnology in cancer therapy and imaging. CA Cancer J Clin 2008;58:97-110.
7. Misra R, Acharya S, Sahoo SK. Cancer nanotechnology: Application of nanotechnology in cancer therapy. Drug Discov Today 2010;15:842-50.
8. Mohanraj VJ, Chen Y. Nanoparticles-a review. Trop J Pharm Res 2006;5:561-73.
9. Wilczewska AZ, Niemirowicz K, Markiewicz KH, Car H. Nanoparticles as drug delivery systems. Pharmacol Rep 2012;64:1020-37.
10. Raj S, Khurana S, Choudhari R, Kesari KK, Kamal MA, Garg N, *et al*. Specific targeting cancer cells with nanoparticles and drug delivery in cancer therapy. Semin Cancer Biol 2021;69:166-77.
11. Pan L, Liu J, Shi J. Cancer cell nucleus-targeting nanocomposites for advanced tumor therapeutics. Chem Soc Rev 2018;47:6930-46.
12. Singh R, Lillard JW Jr. Nanoparticle-based targeted drug delivery. Exp Mol Pathol 2009;86:215-23.
13. Chamundeeswari M, Jeslin J, Verma ML. Nanocarriers for drug delivery applications. Environ Chem Lett 2019;17:849-65.
14. Camargo PH, Satyanarayana KG, Wypych F. Nanocomposites: Synthesis, structure, properties and new application opportunities. Mater Res 2009;12:1-39.
15. Hanafy NA, Leporatti S, El-Kemary M. Mucoadhesive curcumin crosslinked carboxy methyl cellulose might increase inhibitory efficiency for liver cancer treatment. Mater Sci Eng C 2020;116:111119.
16. Basta AH, El-Saied H, El-Deftar MM, El-Henawy AA, El-Sheikh HH, Abdel-Shakour EH, *et al*. Properties of modified carboxymethyl cellulose and its use as bioactive compound. Carbohydr Polym 2016;153:641-51.
17. Rao Z, Ge H, Liu L, Zhu C, Min L, Liu M, *et al*. Carboxymethyl cellulose modified graphene oxide as pH-sensitive drug delivery system. Int J Biol Macromol 2018;107:1184-92.
18. Javanbakht S, Shaabani A. Carboxymethyl cellulose-based oral delivery systems. Int J Biol Macromol 2019;133:21-9.
19. Upadhyaya L, Singh J, Agarwal V, Pandey AC, Verma SP, Das P, *et al*. *In situ* grafted nanostructured ZnO/carboxymethyl cellulose nanocomposites for efficient delivery of curcumin to cancer. J Polym Res 2014;21:550.
20. Premanathan M, Karthikeyan K, Jeyasubramanian K, Manivannan G. Selective toxicity of ZnO nanoparticles toward gram-positive bacteria and cancer cells by apoptosis through lipid peroxidation. Nanomedicine 2011;7:184-92.
21. Akhtar MJ, Ahamed M, Kumar S, Khan MM, Ahmad J, Alrokayan SA. Zinc oxide nanoparticles selectively induce apoptosis in human cancer cells through reactive oxygen species. Int J Nanomedicine 2012;7:845-57.
22. Queirós V, Azeiteiro UM, Soares AM, Freitas R. The antineoplastic drugs cyclophosphamide and cisplatin in the aquatic environment-review. J Hazard Mater 2021;412:125028.
23. Iqubal A, Iqubal MK, Sharma S, Ansari MA, Najmi AK, Ali SM, *et al*. Molecular mechanism involved in cyclophosphamide-induced cardiotoxicity: Old drug with a new vision. Life Sci 2019;218:112-31.
24. Emadi A, Jones RJ, Brodsky RA. Cyclophosphamide and cancer: Golden anniversary. Nat Rev Clin Oncol 2009;6:638-47.
25. Armelao L, Bottaro G, Bovo L, MacCato C, Tondello E, Anselmi F, *et al*. Proteins conjugation with ZnO sol-gel nanopowders. J Solgel Sci Technol 2011;60:352-8.
26. Luna-Martínez JF, Hernández-Uresti DB, Reyes-Melo ME, Guerrero-Salazar CA, González-González VA, Sepúlveda-Guzmán S. Synthesis and optical characterization of ZnS-sodium carboxymethyl cellulose nanocomposite films. Carbohydr Polym 2011;84:566-70.
27. Awan F, Islam MS, Ma Y, Yang C, Shi Z, Berry RM, *et al*. Cellulose nanocrystal-ZnO nanohybrids for controlling photocatalytic activity and UV protection in cosmetic formulation. ACS Omega 2018;3:12403-11.
28. Rigano L, Lionetti N. Nanobiomaterials in galenic formulations and cosmetics. In: Nanobiomaterials in Galenic Formulations and Cosmetics: Applications of Nanobiomaterials. Amsterdam: Elsevier; 2016. p. 121-48.
29. Wolinsky JB, Grinstaff MW. Therapeutic and diagnostic applications of dendrimers for cancer treatment. Adv Drug Deliv Rev 2008;60:1037-55.
30. Pandey H, Rani R, Agarwal V. Liposome and their applications in cancer therapy. Braz Arch Biol Technol 2016;59:e16150477.
31. Akbarzadeh A, Rezaei-Sadabady R, Davaran S, Joo SW, Zarghami N, Hanifehpour Y, *et al*. Liposome: Classification, preparation, and applications. Nanoscale Res Lett 2013;8:102.
32. López-Dávila V, Seifalian AM, Loizidou M. Organic nanocarriers for cancer drug delivery. Curr Opin Pharmacol 2012;12:414-9.
33. Eatemadi A, Daraee H, Karimkhanloo H, Kouhi M, Zarghami N, Akbarzadeh A, *et al*. Carbon nanotubes: Properties, synthesis, purification, and medical applications. Nanoscale Res Lett 2014;9:393.
34. Jagadeesh P, Sowmya K, Radhika PR, Kumar ST. Carbon nanotubes: The future of cancer treatment. Int J Pharma Sci Res 2011;2:217-24.
35. Dragar Č, Potrč T, Nemec S, Roškar R, Pajk S, Kocbek P, *et al*. One-pot method for preparation of magnetic multi-core nanocarriers for drug delivery. Materials (Basel) 2019;12:540.
36. Rivas J, Bañobre-López M, Piñeiro-Redondo Y, Rivas B, López-Quintela MA. Magnetic nanoparticles for application in cancer therapy. J Magn Magn Mater 2012;324:3499-502.

How to cite this article:
Prabha KH, Nannan M, Venkatabalasubramanian S. Preparation of zinc oxide-carboxymethyl cellulose blended with cyclophosphamide for targeted drug delivery to lung adenocarcinoma cells. J App Biol Biotech. 2023;11(Suppl 1):40-45. DOI: 10.7324/JABB.2023.145826